Journal of Fluorescence (2019) 29:399–406
https://doi.org/10.1007/s10895-019-02348-6

ORIGINAL ARTICLE

A Smart Fluorescent Probe Based on Salicylaldehyde Schiff's Base with AIE and ESIPT Characteristics for the Detections of N_2H_4 and ClO^-

Ya Xie[1] · Liqiang Yan[1] · Yujian Tang[1] · Minghui Tang[1] · Shaoyang Wang[1] · Li Bi[1] · Wanying Sun[1] · Jianping Li[2]

Received: 26 September 2018 / Accepted: 14 January 2019 / Published online: 24 January 2019

Abstract

Smart and versatile salicylaldehyde Schiff's bases have been proved their excellent performances including large shocks shift, dual emission wavelengths and sensitive to environment for fluorescence analysis. Herein, a simple salicylaldehyde Schiff's base molecular (**PBAS**) with aggregation-induced emission (AIE) and the excited-state intramolecular proton-transfer (ESIPT) effects was constructed for detecting N_2H_4 and ClO^-. The highly specific and sensitive response to N_2H_4 was witnessed by the fast turn-on of the strong blue fluorescence and to ClO^- was observed by the rapid turn off of the weak green fluorescence simultaneous decomposing of the probe. The results of mass spectrum analysis showed that probe **PBAS** decomposed under the influence of N_2H_4, whereas probe **PBAS** can complex with ClO^- and prevent effective ESIPT process. Benefiting from its high properties, this fluorescence molecular provides an effective tool for probing N_2H_4 and ClO^- in live cells.

Keywords Fluorescence probe · N_2H_4 · ClO^- · Salicylaldehyde · Schiff's bases

Introduction

Hydrazine (N_2H_4) is an important industrial material, which has a wide range of applications in synthetic catalyst, rocket fuel, metal corrosion inhibitor, photographic developer, reducing agent, foaming agent and pharmaceutical intermediate. [1–7] However, N_2H_4 and its aqueous solutions have been confirmed to be highly toxic to humans and animals, which could cause a range of injury to skin, eye, liver and nervous system because of its causticity, acrimony and carcinogenic effect. [8–10]

Hypochlorite (ClO^-) is one of the very important species, which plays a vital role in signaling transmission, body immunity and resist the virus infection in biological cells. [11–13] Nevertheless, too high concentration of ClO^- can cause oxidativestress in biological body, prompting a cascade of diseases like inflammation, pulmonary disease, rheumatism, liver damage, nephropathy, nerve injury and cancer. [14–18] Besides, ClO^- is widely used as decolorizer and disinfector in our daily life, which could greatly increase the concentration of ClO^- in human living environment. Therefore, it is great important to develop convenient methods to investigate the concentrations of N_2H_4 and ClO^- in biological system and in environment.

Fluorescence probe technique has incomparable superiority and competitiveness in the detection of metal ion, anion, protein, pH, viscosity and biochemical process on account of the advantages including convenience, fast, visualization, reliability, real-time imaging, high sensitivity and selectivity. [19] Although a series of fluorescence probes for N_2H_4 and ClO^- have been developed, most of them showed low sensitivity and poor reliability because of the disturbance of aggregation-caused quenching (ACQ). [20, 21] Best of all, AIE phenomenon was found by Tang's group, which solved effectively the thorny ACQ problem. [22–27] It was found that some molecules showed very weak fluorescence in decentralized state in benign solvent, however, their fluorescence greatly improved in aggregate states in poor solvent on account of the restriction of intramolecular rotations process (RIR). [28] AIE molecules

Electronic supplementary material The online version of this article (https://doi.org/10.1007/s10895-019-02348-6) contains supplementary material, which is available to authorized users.

✉ Liqiang Yan
liqiangyan@glut.edu.cn

[1] College of Chemistry and Bioengineering, Guilin University of Technology, Guilin, Guangxi 541004, People's Republic of China

[2] Guangxi Key Laboratory of Electrochemical and Magnetochemical Functional Materials, Guangxi Colleges and Universities Key Laboratory of Food Safety and Detection, Guilin, Guangxi 541004, People's Republic of China

have been successfully used to prepare all kind of excellent biosensors and fluorescence probes. [29]

Aggregation state materials based on ESIPT have a great potential to be used in fluorescence probe and optoelectronic devices because of their unique optical properties like spectral sensitivity to the surrounding medium, dual emission and large Stokes shift owing to the fast structural transform between ketone and enol forms in the excited state. [30–35]

Herein, an AIE luminogenic compound based on 4-(1-pyrrolidinyl)-benzenamine salicylaldehyde (**PBAS**) was developed. **PBAS** molecule can be facilely prepared (Scheme 1). More importantly, it exhibit typical AIE and ESIPT properties and significant fluorescence response to N_2H_4 and ClO^-, which indicated its potential application prospect in fluorescence probe for N_2H_4 and ClO^- sensing.

Experimental

Instrumentation and Materials

NMR spectra were obtained on an AVANCE III HD spectrometer. UV-vis spectra were taken from a Lambda 365 spectrometer (PerkinElmer, America). Fluorescence spectra were obtained by Cary Eclipse fluorescence spectrophotometer (Varian, America). All experimental procedures were carried out at ambient temperature. All reagents were purchased from J&K Scientific as analytical grade, and used directly without secondary purification. Double-distilled water was used to prepare solution throughout the experiment. All of metal ions were prepared from their nitrates. ClO^-, $S_2O_3^{2-}$, $H_2PO_4^-$, F^-, Cl^-, Br^-, ClO_4^-, NO_2^-, HCO_3^- and CO_3^{2-} were respectively prepared from their inorganic salts (NaClO, $Na_2S_2O_3$, NaH_2PO_4, KF, $NaClO_4$, $NaNO_2$, $NaHCO_3$ and Na_2CO_3). O_2^-, $^1O_2$, and ·OH were prepared according the published literatures. [36, 37] Phosphate buffer (PBS) was dissolved in double-distilled water, and was adjusted pH 7.4 with a final concentration at 10 mM.

Synthesis of Probe PBAS

0.70 g (5.0 mmol) of 5-fluorosalicylaldehyde and 0.81 g (5.0 mmol) of 4-(pyrrolidin-1-yl)aniline were dissolved in 30 mL C_2H_5OH. Then the solution was refluxed for 8 h.

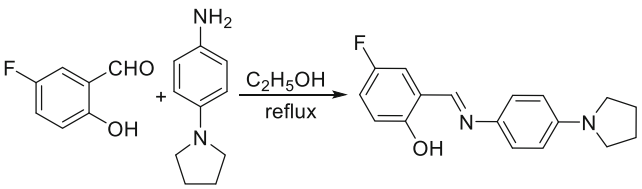

Scheme 1 Synthesis of compound PBAS

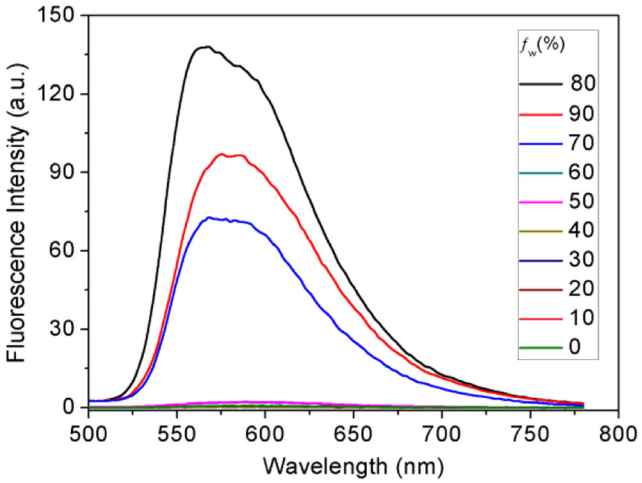

Fig. 1 The emission spectra of probe **PBAS** (30 μM) in DMSO/H_2O mixture solution (λ_{ex}: 400 nm, slit width: 5 nm)

The orange precipitate was filtered out and washed one time with cold C_2H_5OH. Yield: 1.19 g, 83.7%. ^1H NMR (600 MHz, DMSO-d_6) δ (ppm): 1.95–1.98 (m, 4H); 3.26–3.28 (t, $J = 6.0$ Hz, 4H); 6.59, 6.61 (d,$J = 12.0$ Hz, 2H); 6.91, 6.93 (d, $J = 12.0$ Hz, 1H); 7.17–7.20 (m, 1H); 7.34–7.37 (dd, $J = 6.0$ Hz, 2H); 7.40–7.42 (d, $J = 12.0$ Hz, 1H); 8.88 (s, 1H); 13.42 (s, 1H). ^{13}C NMR (150 MHz, DMSO-d_6) δ (ppm): 25.46, 47.86, 112.43, 117.02, 118.06, 119.15, 120.45, 123.16, 135.42, 147.86, 154.57, 156.16, 156.68. ESI-MS, m/z: 285.20 $[M + H]^+$.

General Procedures for the Spectral Measurements

2.5 mL 1.0×10^{-4} M probe in DMSO/PBS buffer solution (1:9, *v*/v, pH 7.4) and 1.0 mL ClO^- or N_2H_4 (dissolved in DMSO/PBS buffer solution) with different concentrations were added into a 25 mL measuring flask, then diluted with

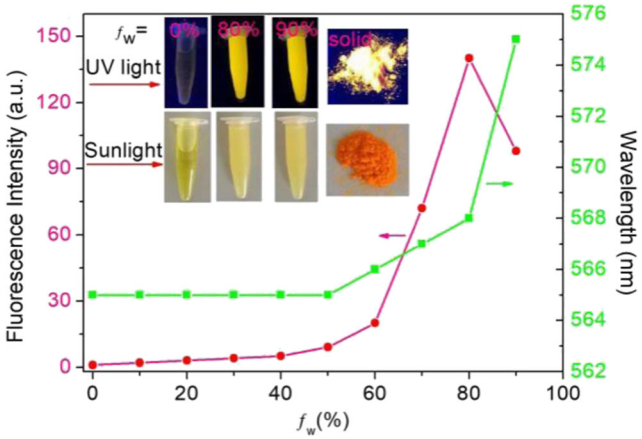

Fig. 2 Fluorescence peaks (violet line) and maximum emission wavelengths (green line) at 570 nm versus f_w for probe 1 (30 μM) (slit width: 5 nm). Inset: probe 1 in the solution state and in the solid state under UV light illumination

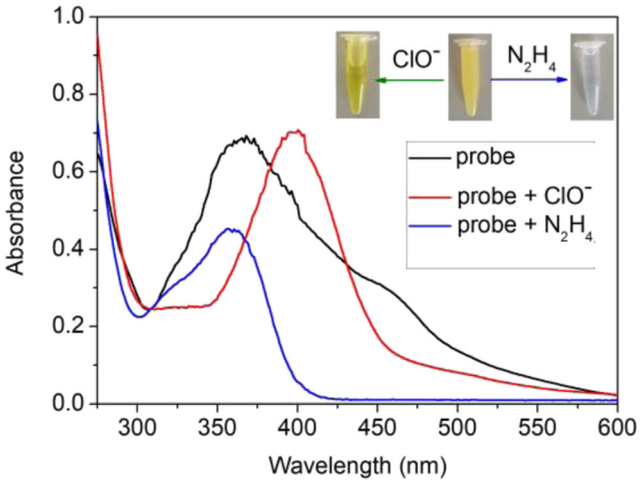

Fig. 3 UV–vis absorption spectra of probe 1 (10 μM) in the absence and presence of ClO^- (10 μM) and N_2H_4 (10 μM). Inset: Color changes of probe 1 upon addition of ClO^- and N_2H_4

the mixture of DMSO/PBS solution (1:9, v/v, pH 7.4) to volume. After equilibrium of 5 min under RT condition, UV-Vis and fluorescence spectra were acquired in quartz cells, respectively. The excitation wavelength (λ_{ex}) of fluorescence spectra was set at 400 nm.

Fluorescence Imaging

A549 cells were purchased from ATCC and were cultivated for 0.5 h with probe **PBAS** (10.0 μM) in DMEM culture at 37 °C, and consequently stained with ClO^- (30.0 μM) or N_2H_4 (30.0 μM) for 10 min under the same conditions. Fluorescence images were performed with an Olympus IX 71 with xenon lamp and Olympus digital camera using blue channel and red channel, respectively.

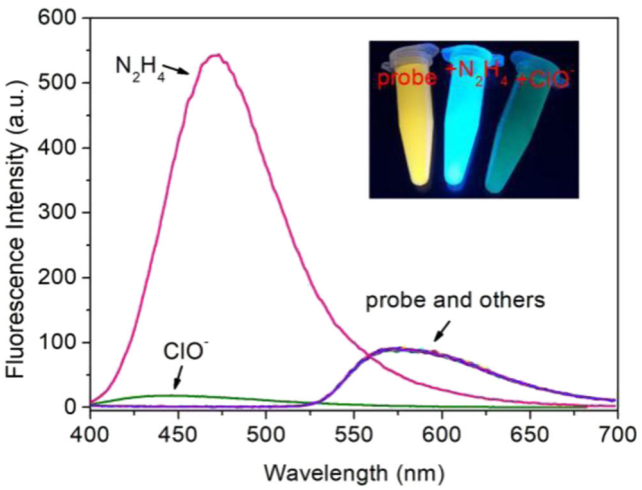

Fig. 4 Fluorescence changes of probe PBAS (10 μM) upon addition of various species (40 μM). Inset: Fluorescence changes excited by a UV lamp upon addition of ClO^- (40 μM) and N_2H_4 (40 μM), respectively

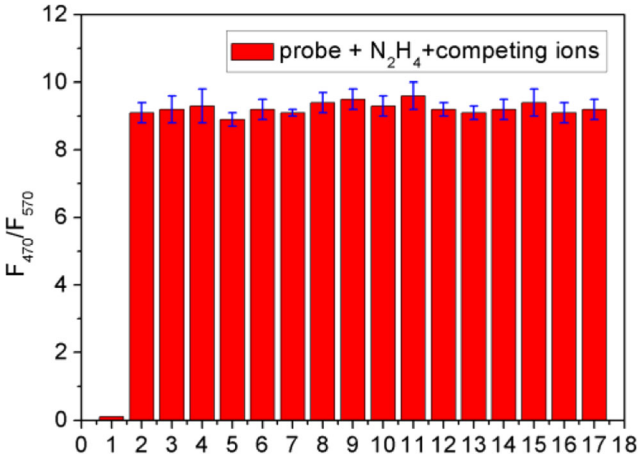

Fig. 5 Fluorescence response of probe **PBAS** (10 μM) in the presence of N_2H_4 (40 μM) and other interference species (40 μM). 1: probe, 2: N_2H_4, 3: $S_2O_3^{2-}$, 4: $H_2PO_4^-$, 5: F^-, 6: Cl^-, 7: Br^-, 8: ClO_4^-, 9: H_2O_2, 10: NO_3^-, 11: SO_3^{2-}, 12: NO_2^-, 13: O_2^-, 14: $^1O_2$, 15:·OH, 16: HCO_3^- and 17: CO_3^{2-}

Results and Discussion

AIE Property

The AIE behavior of **PBAS** in water/DMSO mixture was examined because that **PBAS** molecules tend to be distributed in benign solvent DMSO but would tend to aggregate in water/DMSO mixture with a high water fraction (f_w, vol%). As shown in Figs. 1 and 2, **PBAS** (30.0 μM) shows very weak fluorescence when f_w is less than 60%. When f_w is greater than 70%, fluorescence intensity of **PBAS** solution increased evidently (red line in Fig. 2) and fluorescence peak shifted to 575 nm from 565 nm (green line in Fig. 3). The enhancement of fluorescence can be ascribed to the formation of aggregation, which prevents the nonradiative decay of the molecular energy in excited state by restricting the C=N isomerization

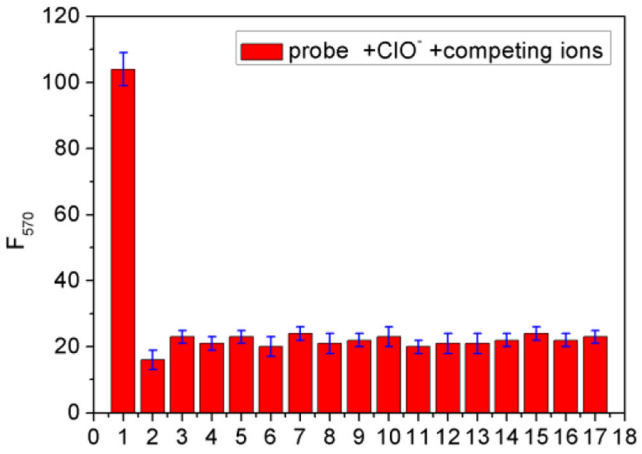

Fig. 6 Fluorescence response of probe PBAS (10 μM) in the presence of ClO^- (40 μM) and other different interferences (40 μM). 1: probe, 2: ClO^-, 3: $S_2O_3^{2-}$, 4: $H_2PO_4^-$, 5: F^-, 6: Cl^-, 7: Br^-, 8: ClO_4^-, 9: H_2O_2, 10: NO_3^-, 11: SO_3^{2-}, 12: NO_2^-, 13: O_2^-, 14: $^1O_2$, 15:·OH, 16: HCO_3^- and 17: CO_3^{2-}

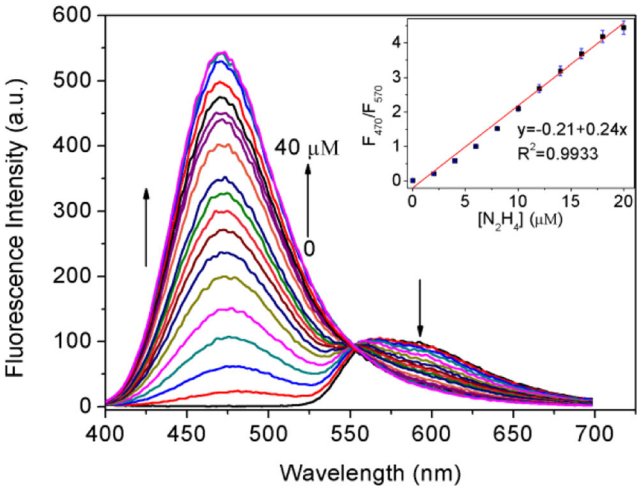

Fig. 7 Fluorescence response of probe **PBAS** (10 μM) upon addition of different concentrations of N_2H_4 (0–40 μM). Inset: plots of emission intensity (F_{470}/F_{570}) against the concentration of N_2H_4

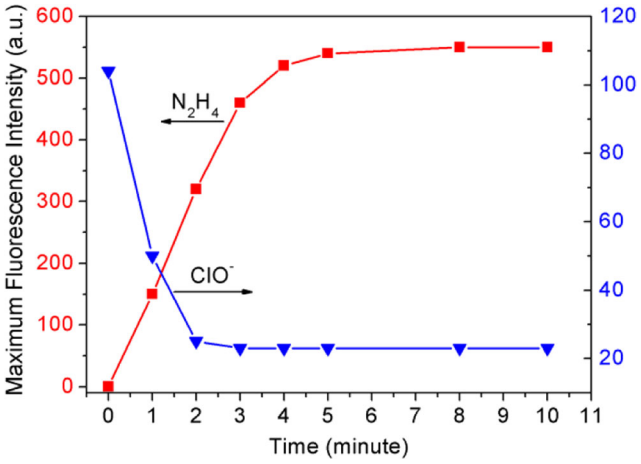

Fig. 9 Time course curves of PBAS fluorescence intensity with addition N_2H_4 (red line) and ClO^- (blue line), respectively

and phenyl group rotation. [38, 39] The red shift phenomena of emission wavelength mainly because that molecular aggregation activated the ESIPT process. [40, 41] The fluorescent molecule based on ESIPT process can exhibit a large Stokes shift caused by the tautomerization between the excited enol form and the excited proton transferred keto form. When f_w is more 90%, fluorescence intensity shows a little decline by reason of the formation of precipitation along with the degree of aggregation increases. These results show that **PBAS** is a typical AIE molecule with ESIPT process.

UV-Vis Absorption Spectra

The UV-vis spectral characteristics of **PBAS** (10 μM) with N_2H_4 and ClO^- were firstly examined in DMSO/PBS solution (1:9, *v*/v, pH 7.4), respectively. As shown in Fig. 1, the absorption peak of **PBAS** at 365 nm disappeared and a new peak at 400 nm appeared after addition of ClO^- (10 μM), and the color of **PBAS** solution changed to deep yellow from light yellow. For another, upon treatment of 10 μM N_2H_4, the absorption peak of **PBAS** at 367 nm decreased and blue shifted to 360 nm. Moreover, a significant color changed from yellow to colorless was easily observed by the naked eye (Fig. 3 inset).

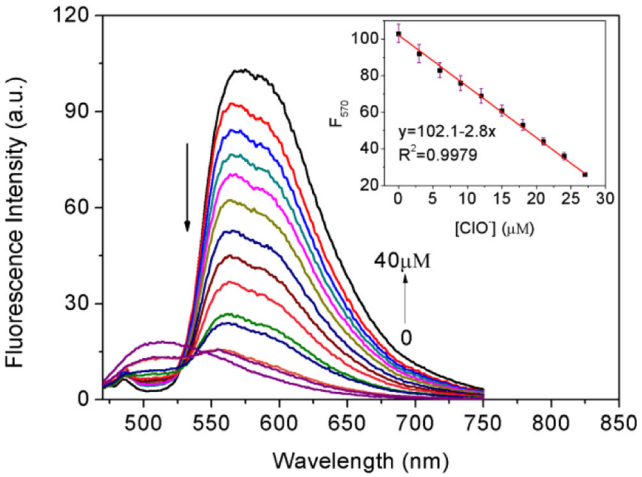

Fig. 8 Fluorescence response of probe **PBAS** (10 μM) upon addition of different concentrations of ClO^- (0–40 μM). Inset: plots of emission intensity (F_{570}) against the concentration of ClO^-

Selectivity of PBAS toward N_2H_4 and ClO^-

To investigate the specific selectivity of compound **PBAS** towards N_2H_4 and ClO^-, a group of competing species such as $S_2O_3^{2-}$, $H_2PO_4^-$, F^-, Cl^-, Br^-, ClO_4^-, H_2O_2, NO_3^-, SO_3^{2-}, NO_2^-, O_2^-, $^1O_2$, ·OH, HCO_3^- and CO_3^{2-} were chosen as the competing species (40 μM) to perform fluorescence experiments. It is found that **PBAS** (10 μM) solution shows strong blue fluorescence with addition of N_2H_4 (40 μM), and displays very weak green fluorescence upon addition of ClO^- (40 μM) as shown in Fig. 4. However, none of the other competing species (40 μM) caused any remarkable change in fluorescence emission under the same condition. The results demonstrate that **PBAS** can be served as a selective fluorescent probe for both N_2H_4 and ClO^- in the presence of other competing species. Furthermore, the interference experiments were also carried out by measuring the fluorescence intensity of **PBAS** (10 μM) in the presence of other metal ions (40 μM) in order to verify the capacity of resisting disturbance of the probe **PBAS**. It can be seen from Fig. 5 that the emission intensity enhancement of **PBAS** is specific towards N_2H_4 and is rarely affected by the presence of other competing species (40 μM). And only ClO^- can effectively cause fluorescence quenching even

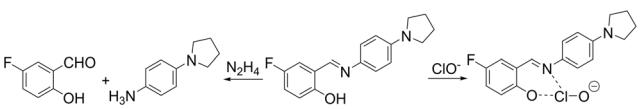

Fig. 10 The proposed detection mechanism of **PBAS** toward N_2H_4 and ClO^-

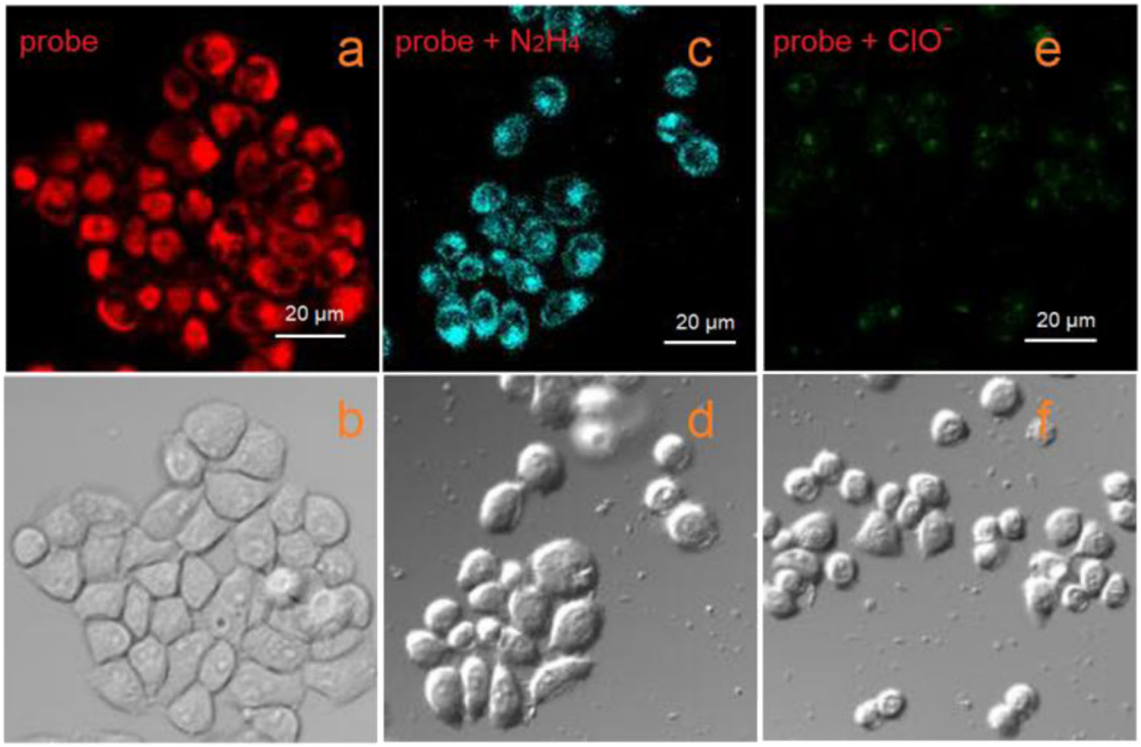

Fig. 11 Fluorescence images of living cells. Fluorescence images, a: probe, c: probe+N_2H_4, e: probe+ClO^-; Bright field: b: probe, d: probe+N_2H_4, f: probe+ClO^-. Scale bar: 20 μM

when other competing species also exit at the same time (Fig. 6).

Fluorescence Spectra of Probe PBAS Titrated with N_2H_4 and ClO^-

The changes in fluorescence spectra of probe **PBAS** with a series concentrations of N_2H_4 (0, 2 μM, 4 μM, 6 μM, 8 μM, 10 μM, 12 μM, 14 μM, 16 μM, 18 μM, 20 μM, 23 μM, 26 μM, 29 μM, 32 μM, 35 μM, 38 μM and 40 μM) were shown in Fig. 7. The fluorescence intensity at 570 nm decreases gradually and disappeared with the improvement of N_2H_4. Meanwhile, a new fluorescence peak at 470 nm comes out and then grows into the maximum emission value. And it is found that the ratios of fluorescence intensities (F_{470}/F_{570}) change from 0.20 to 9.43 when the concentration of N_2H_4 increases from 0 to 40 μM. More importantly, the ratios of the fluorescent intensities versus the concentration of N_2H_4 (from 0 to 20 μM) fit first order linear relation: $y = 0.21 + 0.24x$ ($R^2 = 0.9933$) (Fig. 7 inset). Therefore, probe **PBAS** can detect N_2H_4 by ratiometric fluorescent measurement. Ratiometric fluorescence probe possesses more accurately and sensitively with minimization of the background signal because that it is based on the ratio of two emission intensities instead of the single intensity of one band. [42–45] The detection limit of probe **PBAS** towards N_2H_4 can be calculated as 0.41 μM. [46] The fluorescence changes changes in fluorescence spectra of probe **PBAS** with various amounts of ClO^- (0, 3 μM, 6 μM, 9 μM, 12 μM, 15 μM, 18 μM, 21 μM, 24 μM, 27 μM, 30 μM, 33 μM, 36 μM, 40 μM) were displayed in Fig. 8. The fluorescence intensity at 570 nm gradually weakened with the rising of ClO^- concentration. The fluorescent intensities are linearly proportional to the amount of ClO^- from 0 to 27 μM:

Table 1 The testing results of N_2H_4 and ClO^- concentration in water samples ($n = 3$)

Sample	Sample Number	Addition (μM)	Detection (μM)	Recovery (%)	RSD (%)
N_2H_4	1	5	5.12	102.4	3.16
	2	10	9.88	98.8	2.74
	3	15	15.23	101.5	2.67
ClO^-	1	5	5.31	106.2	4.08
	2	10	10.22	102.2	3.11
	3	15	14.62	97.5	3.62

$y = 102.1–2.8x$ ($R^2 = 0.9979$) (Fig. 8 inset). The detection limit of probe **PBAS** for ClO^- was calculated to be about 0.39 μM. It is conclude that probe **PBAS** has high sensitivity toward N_2H_4 and ClO^-.

Effects of Response Time and pH

Response time is of great significance to verify performance of fluorescent probe. As a consequence, the effect of the reaction time on the response process of probe **PBAS** (10 μM) to N_2H_4 (40 μM) and ClO^- (40 μM) were also carried out as shown in Fig. 9. The investigated results indicate that N_2H_4 interact with **PBAS** within 2 min and after this almost no change in the fluorescence intensity was found along with the time increase up to 10 min. The fluorescence intensity of **PBAS** is closer to the maximum value after interaction with ClO^- within 4 min and then keeps on a steady value in the fluorescence with increased time up to 10 min. This phenomenon provides a strong case that the interaction of **PBAS** with N_2H_4 and ClO^- can be performed directly and rapidly at room temperature, which is important feature for real time detection of N_2H_4 and ClO^-. Moreover, the effect of pH on the detection of N_2H_4 and ClO^- were explored, respectively (Fig. S3). The probe and the probe with N_2H_4 or ClO^- did not show obvious changes of the fluorescence maximum between pH 6.0 and 9.0, which indicated that this probe might be applied to detect N_2H_4 and ClO^- in physiological pH conditions.

Proposed Detection Mechanism

The proposed detection mechanisms of probe **PBAS** to N_2H_4 and ClO^- were investigated by contrasting the mass spectra before and after addition of N_2H_4 and ClO^-, respectively. Along with addition of N_2H_4 in CH_3CN, the molecular ion peak at 285.20 ($[M + H]^+$) disappeared as shown in Fig. S4 and a new peak at 163.20 (Fig. S5) corresponding to [5-fluorosalicylaldehyde+H]$^+$ appeared clearly, which demonstrates that **PBAS** decomposed into 5-fluorosalicylaldehyde. Additionally, after addition of ClO^-, two new peaks at 335.30 and 321.30 respectively corresponding to [**PBAS** + ClO]$^-$ and [**PBAS** + Cl]$^-$ were clearly observed (Fig. S6), which implied the complex **PBAS**-ClO^- formed. According to the mass analyses, the proposed mechanism can be concluded as shown in Fig. 10.

Fluorescence Imaging

To further demonstrate the potential of probe **PBAS** to image N_2H_4 and ClO^- in living cells, we carried out the experiments in living A549 cells. After the cells were incubated with probe **PBAS** (10 μM) for 10 min, strong red fluorescence was exhibited (Fig. 11). When the cells were incubated with N_2H_4 (40 μM) and ClO^- (40 μM) for 30 min, respectively, and then incubated with probe **PBAS** for another 5 min, red fluorescence (Fig. 11a) in living cells was completely replaced with strong blue fluorescence (Fig. 11c) and weak green fluorescence (Fig. 11e). Hence, probe **PBAS** has a good potential application in detection of N_2H_4 and ClO^- using different channels.

Determination of N_2H_4 and ClO^- in Water Samples

In order to investigate the detection performance of **PBAS** to N_2H_4 and ClO^-, probe **PBAS** was firstly applied to detect N_2H_4 and ClO^- in tap water samples. The detection accuracy and relative standard deviation (RSD) was examined by adding a series of known concentrations of standard N_2H_4 and ClO^- to the sample and calculating its recovery. As shown in Table 1, the values of recovery were found from 98.8% to 102.4% of probe **PBAS** to N_2H_4, and from 97.5% to 106.2% of probe **PBAS** to ClO^-. The RSD of **PBAS** to N_2H_4 and ClO^- were from 2.67% to 3.16% and from 3.11% to 4.08%, respectively. The results showed that this probe has a promising potential application for the determination of N_2H_4 and ClO^- in practical application.

Conclusions

In summary, a 5-fluorosalicylaldehy Schiff's base with AIE and ESIPT effects is synthesized. On account of the advantages of high selectivity, excellent sensitivity, ratio fluorescence change, fast response time, and simple construction, **PBAS** can be considered as excellent fluorescence probe for tracking of N_2H_4 and ClO^-. And it is also used for N_2H_4 and ClO^- imaging in live A549 cells.

Acknowledgements This work was supported by College students' innovation and entrepreneurship training program (201810596130), the Natural Science Foundation of Guangxi Province of China (Project No.2015GXNSFFA139005) and High Level Innovation Teams of Guangxi Colleges & Universities and Outstanding Scholars Program (Guijiaoren [2014]49).

References

1. Muzalevskiy VM, Rulev AY, Romanov AR, Kondrashov EV, Ushakov IA, Chertkov VA, Nenajdenko VG (2017) Selective, metal-free approach to 3-or 5-CF3-Pyrazoles: solvent switchable reaction of CF3-Ynones with Hydrazines. J Organomet Chem 82(14):7200–7214. https://doi.org/10.1021/acs.joc.7b00774
2. Tafreshi SS, Roldan A, de Leeuw NH (2017) Micro-kinetic simulations of the catalytic decomposition of hydrazine on the cu(111)

surface. Faraday Discuss 197:41–57. https://doi.org/10.1039/c6fd00186f
3. Serov A, Kwak C (2010) Direct hydrazine fuel cells: a review. Appl Catal B-Environ 98(1–2):1–9. https://doi.org/10.1016/j.apcatb.2010.05.005
4. Ragnarsson U (2001) Synthetic methodology for alkyl substituted hydrazines. Chem Soc Rev 30(4):205–213. https://doi.org/10.1039/B010091a
5. Balsamo A, Macchia B, Macchia F, Rossello A, Giani R, Pifferi G, Pinza M, Broccali G (1983) Synthesis and antibacterial activities of new (alpha-hydrazinobenzyl)cephalosporins. J Med Chem 26(11):1648–1650
6. Ccorahua R, Troncoso OP, Rodriguez S, Lopez D, Torres FG (2017) Hydrazine treatment improves conductivity of bacterial cellulose/graphene nanocomposites obtained by a novel processing method. Carbohydr Polym 171:68–76. https://doi.org/10.1016/j.carbpol.2017.05.005
7. Jana MK, Gupta U, Rao CNR (2016) Hydrazine as a hydrogen carrier in the photocatalytic generation of H-2 using CdS quantum dots. Dalton T 45(38):15137–15141. https://doi.org/10.1039/c6dt02505f
8. Kerai MDJ, Timbrell JA (1997) Effect of fructose on the biochemical toxicity of hydrazine in isolated rat hepatocytes. Toxicology 120(3):221–230. https://doi.org/10.1016/S0300-483x(97)00059-0
9. Waterfield CJ, Turton JA, Scales MDC, Timbrell JA (1993) Investigations into the effects of various hepatotoxic compounds on urinary and liver taurine levels in rats. Arch Toxicol 67(4):244–254. https://doi.org/10.1007/Bf01974343
10. Garrod S, Bollard ME, Nicholllst AW, Connor SC, Connelly J, Nicholson JK et al (2005) Integrated metabonomic analysis of the multiorgan effects of hydrazine toxicity in the rat. Chem Res Toxicol 18(2):115–122. https://doi.org/10.1021/tx0498915
11. Dickinson BC, Huynh C, Chang CJ (2010) A palette of fluorescent probes with varying emission colors for imaging hydrogen peroxide signaling in living cells. J Am Chem Soc 132(16):5906–5915. https://doi.org/10.1021/ja1014103
12. Yue YK, Huo FJ, Yin CX, Escobedo JO, Strongin RM (2016) Recent progress in chromogenic and fluorogenic chemosensors for hypochlorous acid. Analyst 141(6):1859–1873. https://doi.org/10.1039/c6an00158k
13. Yap YW, Whiteman M, Cheung NS (2007) Chlorinative stress: An under appreciated mediator of neurodegeneration? Cell Signal 19(2):219–228. https://doi.org/10.1016/j.cellsig.2006.06.013
14. Pattison DI, Davies MJ (2006) Evidence for rapid inter- and intramolecular chlorine transfer reactions of histamine and carnosine chloramines: implications for the prevention of hypochlorous-acid-mediated damage. Biochemistry-Us 45(26):8152–8162. https://doi.org/10.1021/bi060348s
15. Malle E, Buch T, Grone HJ (2003) Myeloperoxidase in kidney disease. Kidney Int 64(6):1956–1967. https://doi.org/10.1046/j.1523-1755.2003.00336.x
16. Steinbeck MJ, Nesti LJ, Sharkey PF, Parvizi J (2006) Myeloperoxidase and chlorinated-peptides in osteoarthritis: potential biomarkers of the disease. J Bone Miner Res 21:S144–S144
17. Maruyama Y, Lindholm B, Stenvinkel P (2004) Inflammation and oxidative stress in ESRD - the role of myeloperoxidase\. J Nephrol 17:S72–S76
18. Sam CH, Lu HK (2009) The role of hypochlorous acid as one of the reactive oxygen species in periodontal disease. J Dent Sci 4(2):45–54. https://doi.org/10.1016/S1991-7902(09)60008-8
19. Yan LQ, Ma Y, Cui MF, Qi ZJ (2015) A novel coumarin-based fluorescence chemosensor containing L-histidine for aluminium(III) ions in aqueous solution. Anal Methods-Uk 7(15):6133–6138. https://doi.org/10.1039/c5ay01466b
20. Thomas SW, Joly GD, Swager TM (2007) Chemical sensors based on amplifying fluorescent conjugated polymers. Chem Rev 107(4):1339–1386. https://doi.org/10.1021/cr0501339
21. Grimsdale AC, Chan KL, Martin RE, Jokisz PG, Holmes AB (2009) Synthesis of light-emitting conjugated polymers for applications in electroluminescent devices. Chem Rev 109(3):897–1091. https://doi.org/10.1021/cr000013v
22. Luo JD, Xie ZL, Lam JWY, Cheng L, Chen HY, Qiu CF et al (2001) Aggregation-induced emission of 1-methyl-1,2,3,4,5-pentaphenylsilole. Chem Commun 18:1740–1741. https://doi.org/10.1039/B105159h
23. Yuan WZ, Chen SM, Lam JWY, Deng CM, Lu P, Sung HHY, Williams ID, Kwok HS, Zhang Y, Tang BZ (2011) Towards high efficiency solid emitters with aggregation-induced emission and electron-transport characteristics. Chem Commun 47(40):11216–11218. https://doi.org/10.1039/c1cc14122h
24. Zhao ZJ, Geng JL, Chang ZF, Chen SM, Deng CM, Jiang T, Qin W, Lam JWY, Kwok HS, Qiu H, Liu B, Tang BZ (2012) A tetraphenylethene-based red luminophor for an efficient non-doped electroluminescence device and cellular imaging. J Mater Chem 22(22):11018–11021. https://doi.org/10.1039/c2jm31482g
25. Yan LQ, Li RJ, Shen W, Qi ZJ (2018) Multiple-color AIE coumarin-based Schiff bases and potential application in yellow OLEDs. J Lumin 194:151–155. https://doi.org/10.1016/j.jlumin.2017.10.032
26. Gui SL, Huang YY, Hu F, Jin YL, Zhang GX, Yan LS, Zhang D, Zhao R (2015) Fluorescence turn-on Chemosensor for highly selective and sensitive detection and bioimaging of Al3+ in living cells based on ion-induced aggregation. Anal Chem 87(3):1470–1474. https://doi.org/10.1021/ac504153c
27. Zhao N, Gong Q, Zhang RX, Yang J, Huang ZY, Li N, Tang BZ (2015) A fluorescent probe with aggregation-induced emission characteristics for distinguishing homocysteine over cysteine and glutathione. J Mater Chem C 3(32):8397–8402. https://doi.org/10.1039/c5tc01159k
28. Hong YN, Lam JWY, Tang BZ (2011) Aggregation-induced emission. Chem Soc Rev 40(11):5361–5388. https://doi.org/10.1039/c1cs15113d
29. Mei J, Leung NLC, Kwok RTK, Lam JWY, Tang BZ (2015) Aggregation-induced emission: together we Shine, united we soar! Chem Rev 115(21):11718–11940. https://doi.org/10.1021/acs.chemrev.5b00263
30. Yan LQ, Qing TT, Li RJ, Wang ZW, Qi ZJ (2016) Synthesis and optical properties of aggregation-induced emission (AIE) molecules based on the ESIPT mechanism as pH- and Zn2+−responsive fluorescent sensors. RSC Adv 6(68):63874–63879. https://doi.org/10.1039/c6ra09920c
31. Yan LQ, Kong ZN, Xia Y, Qi ZJ (2016) A novel coumarin-based red fluorogen with AIE, self-assembly, and TADF properties. New J Chem 40(8):7061–7067. https://doi.org/10.1039/c6nj01296e
32. Padalkar VS, Seki S (2016) Excited-state intramolecular proton-transfer (ESIPT)-inspired solid state emitters. Chem Soc Rev 45(1):169–202. https://doi.org/10.1039/c5cs00543d
33. Wang EJ, Lam JWY, Hu RR, Zhang C, Zhao YS, Tang B (2014) Twisted intramolecular charge transfer, aggregation-induced emission, supramolecular self-assembly and the optical waveguide of barbituric acid-functionalized tetraphenylethene. J Mater Chem C 2(10):1801–1807. https://doi.org/10.1039/c3tc32161d
34. Yan LQ, Kong ZN, Shen W, Du WQ, Zhou Y, Qi ZJ (2016) An aggregation-induced emission (AIE) ratiometric fluorescent cysteine probe with an exceptionally large blue shift. RSC Adv 6(7):5636–5640. https://doi.org/10.1039/c5ra22245a
35. An BK, Kwon SK, Jung SD, Park SY (2002) Enhanced emission and its switching in fluorescent organic nanoparticles. J Am Chem Soc 124(48):14410–14415. https://doi.org/10.1021/ja0269082
36. Kubo Y, Yamamoto M, Ikeda M, Takeuchi M, Shinkai S, Yamaguchi S, Tamao K (2003) A colorimetric and ratiometric fluorescent chemosensor with three emission changes: fluoride

ion sensing by a triarylborane-porphyrin conjugate. Angew Chem Int Ed 42(18):2036–2040. https://doi.org/10.1002/anie.200250788

37. Zhang X, Yan YC, Hang YD, Wang J, Hua JL, Tian H (2017) A phenazine-barbituric acid based colorimetric and ratiometric near-infrared fluorescent probe for sensitively differentiating biothiols and its application in TiO2 sensor devices. Chem Commun 53(42):5760–5763. https://doi.org/10.1039/c7cc01925d
38. Li XH, Zhang GX, Ma HM, Zhang DQ, Li J, Zhu DB (2004) 4,5-Dimethylthio-4′-[2-(9-anthryloxy)ethylthio]tetrathiafulvalene, a highly selective and sensitive chemiluminescence probe for singlet oxygen. J Am Chem Soc 126(37):11543–11548. https://doi.org/10.1021/ja0481530
39. Koide Y, Urano Y, Hanaoka K, Terai T, Nagano T (2011) Development of an Si-rhodamine-based far-red to near-infrared fluorescence probe selective for Hypochlorous acid and its applications for biological imaging. J Am Chem Soc 133(15):5680–5682. https://doi.org/10.1021/ja111470n
40. Ma Z, Sun W, Chen LZ, Li J, Liu ZZ, Bai HX, Zhu M, du L, Shi X, Li M (2013) A novel hydrazino-substituted naphthalimide-based fluorogenic probe for tert-butoxy radicals. Chem Commun 49(56):6295–6297. https://doi.org/10.1039/c3cc42052c
41. Wu JS, Liu WM, Zhuang XQ, Wang F, Wang PF, Tao SL, Zhang XH, Wu SK, Lee ST (2007) Fluorescence turn on of coumarin derivatives by metal cations: a new signaling mechanism based on C=N isomerization. Org Lett 9(1):33–36. https://doi.org/10.1021/ol062518z
42. Jiang GY, Zeng GJ, Zhu WP, Li YD, Dong XB, Zhang GX, Fan X, Wang J, Wu Y, Tang BZ (2017) A selective and light-up fluorescent probe for beta-galactosidase activity detection and imaging in living cells based on an AIE tetraphenylethylene derivative. Chem Commun 53(32):4505–4508. https://doi.org/10.1039/c7cc00249a
43. Cui GL, Lan ZG, Thiel W (2012) Intramolecular hydrogen bonding plays a crucial role in the Photophysics and photochemistry of the GFP chromophore. J Am Chem Soc 134(3):1662–1672. https://doi.org/10.1021/ja208496s
44. Xiao HD, Chen K, Cui DD, Jiang NN, Yin G, Wang J, Wang R (2014) Two novel aggregation-induced emission active coumarin-based Schiff bases and their applications in cell imaging. New J Chem 38(6):2386–2393. https://doi.org/10.1039/c3nj01557b
45. Xu C, Li HD, Yin BZ (2015) A colorimetric and ratiometric fluorescent probe for selective detection and cellular imaging of glutathione. Biosens Bioelectron 72:275–281. https://doi.org/10.1016/j.bios.2015.05.030
46. Zhu BC, Zhang XL, Li YM, Wang PF, Zhang HY, Zhuang XQ (2010) A colorimetric and ratiometric fluorescent probe for thiols and its bioimaging applications. Chem Commun 46(31):5710–5712. https://doi.org/10.1039/c0cc00477d